# Enhanced Brain Tumor Classification from MRI Images Using Deep Learning Model

**Conference Paper** · December 2023

DOI: 10.1109/ICCIT60459.2023.10441064



**5 authors**, including:

Asadullah Bin Rahman
Hajee Mohammad Danesh Science and Technology University
**1** PUBLICATION **0** CITATIONS
SEE PROFILE

Md. Touhid Islam
Hajee Mohammad Danesh Science and Technology University
**14** PUBLICATIONS **29** CITATIONS
SEE PROFILE

Md Rashedul Islam
Deakin University
**42** PUBLICATIONS **297** CITATIONS
SEE PROFILE

Md Sohrawordi
Hajee Mohammad Danesh Science and Technology University
**18** PUBLICATIONS **104** CITATIONS
SEE PROFILE

2023 26th International Conference on Computer and Information Technology (ICCIT)
13-15 December, Cox's Bazar, Bangladesh

# Enhanced Brain Tumor Classification from MRI Images Using Deep Learning Model

Asadullah Bin Rahman[1], Md. Touhid Islam[2*], Md. Rashedul Islam[3], Md. Sohrawordi[4], Md. Nahid Sultan[5]
[1,2,3,4,5]Department of Computer Science and Engineering, Hajee Mohammad Danesh Science and Technology University
Dinajpur-5200, Bangladesh
[1]galib.hstu.cse17@gmail.com, [2]shourovhstu17@gmail.com, [3]rashedul_cse@hstu.ac.bd,
[4]mdsohrawordi@hstu.ac.bd, [5]nahid.sultan@hstu.ac.bd

***Abstract*—In the realm of image classification, traditional algorithms, encompassing both machine learning and deep learning, grapple with formidable challenges arising from uneven pixel ranges and dimensionality reduction. This results in a significant impediment to achieving accurate image categorization. Numerous examples of such traditional methods, including KNN, Random Forest, SVM, DNN, CNN etc, have encountered persistent issues such as inefficient performance of feature engineering, limited accuracy, etc. In response to these challenges, this paper introduces a novel image classification method that integrates pixel mapping, DWT, and CNN for improved efficiency and reliability. By resolving irregular pixel ranges through initial pixel mapping, our method establishes uniformity as a foundation for subsequent image analysis. Subsequently, DWT is employed to dissect and reduce image dimensionality, extracting essential features while lowering computational complexity. This two-step preprocessing approach forms a robust foundation for effective data classification. Within this framework, our proposed CNN architecture plays a pivotal role, utilizing both spectral and spatial information to address image categorization challenges. The network's capacity to learn complex patterns enhances classification accuracy. In extensive evaluations, our methodology surpasses conventional classification techniques, yielding impressive results. With an Overall Accuracy (OA) of 96.9% and a Kappa statistic of 95.16%, our method showcases excellence and practical potential. These compelling achievements underscore the significance of our approach in tackling image classification challenges, paving the way for enhanced precision and efficiency across various domains.**

***Index Terms*—Contrast Enhanced MRI(CE-MRI), Brain Tumor, Discrete Wavelet Transformation(DWT), CNN**

## I. Introduction

Brain tumors are abnormal brain or spinal cord cell growth that can cause serious health problems and even death. According to the American Cancer Society, about 24,810 brain or spinal cord malignant tumors will be diagnosed in the United States in 2023, and about 18,990 people will die [1]. Globally, brain tumors are estimated to affect over 250,000 people and cause over 250,000 deaths each year [2]. On average, brain tumors reduce life expectancy by 27 years, which is the highest among all cancers [3]. Early diagnosis of brain tumors is crucial for improving patients' chances of survival and quality of life. However, diagnosing brain tumors can be challenging because of their diversity, complexity, and variability. Moreover, some brain tumors may not cause symptoms until they are substantial or have spread to other brain parts. Computer scientists can assist in tumor detection by developing and applying advanced techniques such as image processing, machine learning, and artificial intelligence. These techniques can help analyze medical images such as magnetic resonance imaging (MRI) or computed tomography (CT) scans and extract useful information such as tumor size, shape, location, type, and grade. This information can help doctors make more accurate and timely diagnoses and plan appropriate treatments for patients.

In recent times, extensive research has been conducted in the field of automated brain tumor classification. Das et al. [4] introduced preprocessing techniques as a preliminary step before the classification task. They performed operations such as resizing, histogram equalization, and gaussian filtering on the input data before feeding it into the Convolutional Neural Network (CNN). One notable omission in their work concerns the handling of image pixel values. As evidenced in Fig. 2b of their paper, a significant number of pixel values are set to 255. This phenomenon occurs when the pixel range is saturated, i.e., everything below 0 becomes 0, and everything above 255 becomes 255. Correctly mapping these pixel values, as demonstrated in our alternative experiment, resulted in improved performance. Sejuti et al. [5] presented two distinct approaches: i) a CNN model and ii) a CNN-SVM Hybrid model. Notably, they did not employ any preprocessing techniques. Their hybrid model exhibited superior performance than the CNN model. Swati et al. [6] proposed a deep learning model, VGG19, and conducted blockwise fine-tuning. It is worth noting that their model is complex and demands significant computational resources. Despite these challenges, their method achieved impressive accuracy. Tonmoy et al. [7] focused on binary classification using the BRATS dataset. They introduced two distinct approaches: i) extracting statistical features and employing six traditional classifiers and ii) utilizing a CNN model. The Support Vector Machine (SVM) performed best among the traditional classifiers. On the other hand, their CNN model outperformed the traditional methods. However, we got slightly lower accuracy when experimenting with their CNN method with the figshare [8] multi-classification dataset. Mallick et al. [9] proposed a novel method that uses a deep wavelet autoencoder (DWA) to extract features from the MRI images and a deep neural network (DNN) to perform the classification on the RIDER Neuro MRI [10] dataset. The paper explains that the DWA

979-8-3503-5901-5/23/$31.00 ©2023 IEEE

is a type of unsupervised learning algorithm that can learn hierarchical representations of the data by applying wavelet transforms and encoding-decoding operations. The paper states that the DWA can capture both the spatial and frequency information of the images and reduce the dimensionality and noise of the data. The paper also describes the architecture and parameters of the DNN, which consists of three hidden layers and a softmax output layer. The paper claims that the DNN can learn complex nonlinear relationships between the features and the labels and achieve high accuracy and generalization.

Discrete Wavelet Transformation (DWT) is proposed because of the image compression task. It is a powerful mathematical tool used in signal processing and data analysis. DWT decomposes a signal or data series into various frequency components, or "wavelets". This process provides a multiresolution representation of the original data, which can be used for a wide range of purposes, such as denoising, image compression, and feature extraction. Throughout DWT, the input data undergoes a series of filtering and downsampling operations. The high-pass and low-pass filters are applied alternately to extract high-frequency and low-frequency components. Ultimately, DWT produces a collection of approximation and detail coefficients at each level of decomposition, offering a comprehensive view of the data.

The proposed model has distinct features that set it apart from any previous methods:

1) Effectively addresses irregular pixel ranges through pixel mapping, ensuring consistent and reliable data processing.
2) Utilizing DWT, the technique decomposes images and significantly reduces their dimensionality, facilitating efficient data analysis and classification.
3) A robust Convolutional Neural Network (CNN) is implemented to efficiently perform classification tasks, harnessing the power of deep learning for accurate image analysis.

In the following sections, we will discover more about our strategy. In section II, we discuss how we processed the images and the architecture of our CNN model. Section III presents an in-depth analysis of the dataset, the applied parameters, model comparison, and discussion. In the final section IV, we conclude with possible future works.

## II. Proposed Methodology

We prepared the images by scaling and compressing them using Discrete Wavelet Transformation. Then, we trained our CNN model and compared it with other models for performance evaluation. The steps are shown in Fig. 1.

### A. Preprocessing

Medical images are DICOM by nature. Though the images were processed and converted into MATLAB file format, we processed them again to fit the best for CNN. As the images

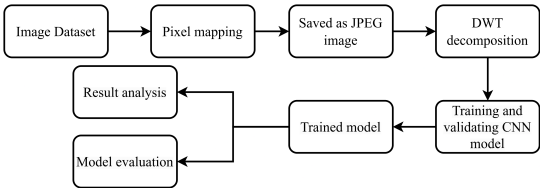


Fig. 1. Proposed methodology for classification using CNN

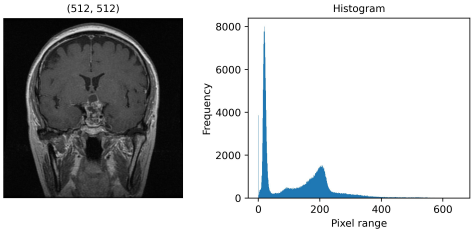


(a) Actual Image ($512 \times 512$)

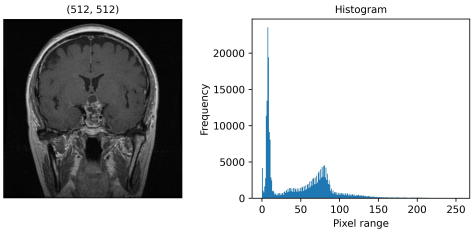


(b) Rescaled Image ($512 \times 512$)

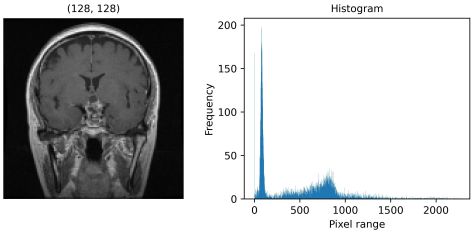


(c) DWT Compressed Image ($128 \times 128$)

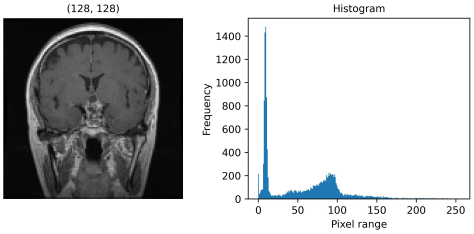


(d) DWT Compressed & Rescaled Image ($128 \times 128$)

Fig. 2. Histogram Analysis of an MRI image from Dataset

are in int16 format (see Fig. 2a), we rescaled those in uint8 and saved them as jpg images (see Fig. 2b).

$$scaled\_img = \frac{img - \min(img)}{\max(img) - \min(img)} \times 255 \qquad (1)$$

Instead of directly resizing the images into $128 \times 128$, we compressed the image to $128 \times 128$ using Discrete Wavelet Transformation. As the pixel range becomes irregular after

compression(see Fig. 2c), we scaled again into 0-255 (Fig. 2d). That is how we achieved both the ideal dimension and the pixel range.

We implemented $haar$ wavelet with $periodization$ mode and performed 2-level DWT decomposition. First, the input image is decomposed into four sets of coefficients: $cA_1$(approximation coefficient 1), $cH_1$(horizontal detailed coefficient 1), $cV_1$(vertical detailed coefficient 1), and $cD_1$(diagonal detailed coefficient 1). The approximation coefficient 1 ($cA_1$) becomes $256 \times 256$ dimension, and as the name suggests, other coefficients hold the positional information. Next, we decomposed the approximation coefficient 1 ($cA_1$) into four sets of coefficients($cA_2$, $cH_2$, $cV_2$, $cD_2$). The $cA_2$ is reduced to $128 \times 128$, which we used as input in our model. The decomposition is shown in Fig. 3 and 4.

### B. Convolutional Neural Network(CNN)

CNNs, or Convolutional Neural Networks, work similarly to the human eye by scanning and collecting information from images. The network is made up of multiple convolutional layers that gather image features, with polling layers added to decrease the number of features and computations required [11]. After several rounds of convolution and pooling, only the crucial features are selected, and the entire feature set is flattened to feed the neural networks that do the classification [12]. That is the basic workflow of a CNN. The operations that take place in the CNN is mentioned as follows:

Conv2D: The convolution operation involves sliding a filter (a 2D matrix) over the input and computing the element-wise product and sum of the overlapping values [13]. The result is another 2D matrix called a feature map.

$$y_{i,j} = \sum_{m=0}^{M-1} \sum_{n=0}^{N-1} x_{i+m,j+n} f_{m,n} \tag{2}$$

where x is the input, f is the filter, y is the feature map, and M and N are the filter dimensions.

MaxPooling2D: The feature is downsampled by the pooling operations.

$$\hat{y}_{i,j} = \max_{m=iS}^{iS+P-1} \max_{n=jS}^{jS+P-1} x_{m,n} \tag{3}$$

where x is the feature map, $\hat{y}$ is the pooled output, P is the pooling size, and S is the stride.

Flatten: This layer reshapes the pooled output into a one-dimensional vector, which can be fed into a dense layer.

Dense: This layer performs a linear transformation on the flattened vector, followed by an activation function. Here, x is the flattened vector, W is a weight matrix, b is a bias vector, $\sigma$ is an activation function, and y is the output vector.

$$y = \sigma(Wx + b) \tag{4}$$

ReLU: This is an activation function that applies a non-linear transformation to the input. Here, x is the input and $\sigma$(x) is the output.

$$\sigma(x) = \max(0, x) \tag{5}$$

Softmax: This is an activation function that normalizes the input vector into a probability distribution. Here, $x_i$ is the i-th element of the input vector, $\sigma(x_i)$ is the i-th element of the output vector, and K is the size of the vector.

$$\sigma(x_i) = \frac{e^{x_i}}{\sum_{j=1}^{K} e^{x_j}} \tag{6}$$

However, our CNN model comprises nine layers, including three pairs of Convolutional 2D and Maxpooling 2D layers, followed by a flattening layer. At the top, there are two dense layers with 512 and 3 nodes, separated by a dropout layer (0.5 rate). ReLU activation functions are used in Convolutional and the first dense layers, while Softmax is used in the final dense layer for probability estimation. Each Convolutional layer uses a $3 \times 3$ kernel, and Maxpooling layers have a $2 \times 2$ pool size. Filter counts in Convolutional layers are 32, 32, and 64. Total trainable parameters are outlined in Table I.

TABLE I
BRIEFLY SUMMARIZED PROPOSED CNN MODEL LAYERS

| Layer (type) | Output | Parameters |
|---|---|---|
| Conv1 (Conv2D) | (None, 126, 126, 32) | 320 |
| Max_Pool_1 (MaxPooling2D) | (None, 63, 63, 32) | 0 |
| Conv2 (Conv2D) | (None, 61, 61, 32) | 9248 |
| Max_Pool_2 (MaxPooling2D) | (None, 30, 30, 32) | 0 |
| Conv3 (Conv2D) | (None, 28, 28, 64) | 18496 |
| Max_Pool_3 (MaxPooling2D) | (None, 14, 14, 64) | 0 |
| flatten (Flatten) | (None, 12544) | 0 |
| fc1 (Dense) | (None, 512) | 6423040 |
| dropout (Dropout) | (None, 512) | 0 |
| fc2 (Dense) | (None, 3) | 1539 |
| Total trainable parameters: 6,452,643, Non-trainable parameters: 0 | | |

## III. DATASET AND RESULT ANALYSIS

### A. Experimental Data

The dataset [8] is a collection of 3064 T1-weighted Contrast Enhanced Magnetic Resonance Image from 233 patients. It was acquired between 2005 and 2010 from different medical colleges in China. The dataset consists of 708 Meningioma, 930 Pituitary and 1426 Glioma tumor images. The images are in MATLAB data format. This dataset is ideal for classification and segmentation tasks as it contains image data, tumor border, tumor mask, and label. As we did classification, we used only images and labels.

### B. Experimental Configuration

As part of our training process, we made some adjustments to the pixel values to ensure they fell within the 0-1 range, which greatly simplified computations. We also incorporated various image transformations like zooming, shearing, and flipping while training to prevent overfitting. To achieve this, we employed the ImageDataGenerator class from the Keras library for real-time data augmentation. Initially, the learning rate was set to 0.01, but if five consecutive epochs showed no noticeable reduction in validation loss, we reduced the learning rate by 80% of the previous rate. Finally, we conducted this study on Google Colab using the Tensorflow and Keras framework.

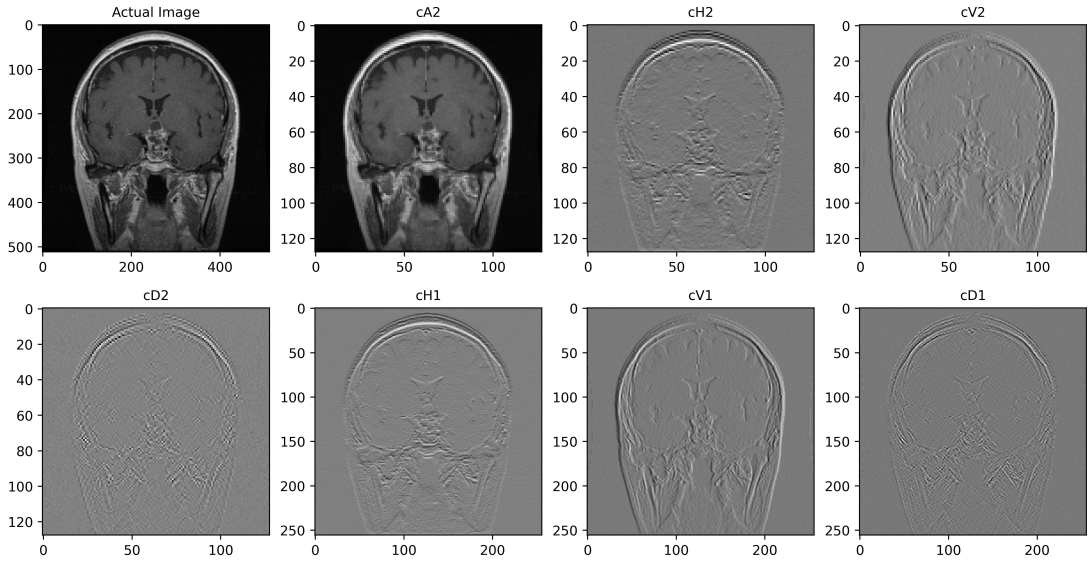


Fig. 3. Image with DWT coefficients for compact data representation

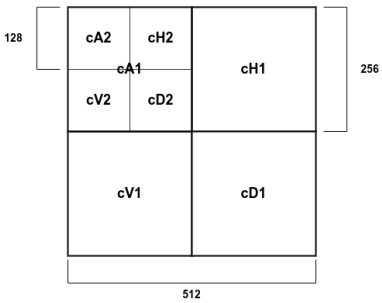


Fig. 4. Image Decomposition using DWT

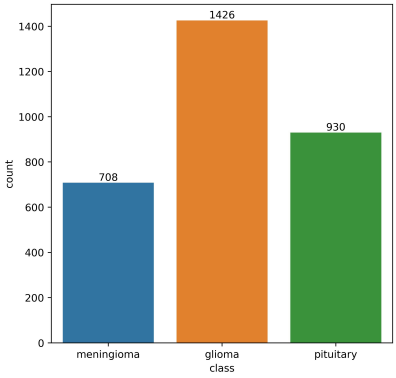


Fig. 5. Number of samples of each class in the dataset

### C. Hyper Parameters

In our experiment, 20% of the dataset(613 images) was selected for final evaluation. From the rest 80%(2451 images) data, 10%(245 images) was used for validation in each epoch, while the remaining 90%(2206 images) was used for training the model. The training parameters are shown in Table II.

TABLE II
PARAMETERS USED IN PROPOSED METHOD

| | | |
|---|---|---|
| **Image Augmentation Parameters** | i. Rescale | 1./255 |
| | ii. Fill mode | nearest |
| | iii. Shear range | 0.2 |
| | iv. Zoom range | 0.2 |
| | v. Horizontal flip | True |
| **Model Parameters** | i. Epoch | 100 |
| | ii. ReduceLROnPlateau | Factor 0.8 |
| | | Patience 5 |
| | | Cooldown 1 |
| | | Min lr 1.00E-04 |
| | | Monitor val_loss |

### D. Performance Evaluation

Our model's performance is evaluated using overall accuracy, average accuracy, precision, sensitivity, specificity, kappa, and ROC curve. The ROC curve shows the trade-off between true positive rate and false positive rate as the threshold changes, and AUC measures how well a binary classifier distinguishes between two classes. The ROC OvR method is used to evaluate multiclass models by comparing each class against all others. This converts the multiclass classification into a binary classification for evaluation.

### E. Result Discussion

Our Convolutional Neural Network (CNN) was trained using 2206 images. Each training batch consisted of 32 images, necessitating 69 iterations to complete a single epoch. Throughout training, our primary criterion for model selection was the validation loss. The lowest validation loss occurred at epoch 61, yielding a remarkable value of 0.06961, coupled with an impressive validation accuracy of 0.9673. Subsequently, despite efforts to fine-tune our model by reducing the learning rate and extending training for an additional 29 epochs, we were unable to surpass this validation loss.

TABLE III
PERFORMANCE COMPARISON WITH VARIOUS STATE OF THE ART METHODS

| Method | Metrics | | | | Class | | |
|---|---|---|---|---|---|---|---|
| | Accuracy(%) | | | Others | Meningioma | Glioma | Pituitary |
| | OA | AA | Kappa | | | | |
| Pixel saturation → Gaussian filtering→ Histogram Equalization + CNN [4] | 91.85 | 90.6 | 85.68 | Sensitivity | 0.94 | 0.84 | 0.98 |
| | | | | Precision | 0.79 | 0.96 | 0.95 |
| | | | | Specificity | 0.97 | 0.88 | 0.99 |
| CNN-1 [5] | 90.23 | 88.83 | 84.53 | Sensitivity | 0.76 | 0.91 | 0.99 |
| | | | | Precision | 0.8 | 0.9 | 0.97 |
| | | | | Specificity | 0.934 | 0.917 | 0.995 |
| CNN + SVM [5] | 92.83 | 90.92 | 88.59 | Sensitivity | 0.78 | 0.96 | 0.99 |
| | | | | Precision | 0.88 | 0.93 | 0.96 |
| | | | | Specificity | 0.939 | 0.96 | 0.995 |
| VGG19 + Fine Tuning [6] | 94.29 | 93.84 | 91.09 | Sensitivity | 0.9 | 0.96 | 0.95 |
| | | | | Precision | 0.88 | 0.95 | 1 |
| | | | | Specificity | 0.967 | 0.962 | 0.981 |
| CNN-2 [7] | 90.38 | 88.33 | 84.76 | Sensitivity | 0.7 | 0.96 | 0.99 |
| | | | | Precision | 0.9 | 0.87 | 0.96 |
| | | | | Specificity | 0.905 | 0.966 | 0.995 |
| Experiment 1: Pixel Mapping → Gaussian filtering → Histogram Equalization + CNN | 94 | 93.32 | 90.66 | Sensitivity | 0.86 | 0.96 | 0.98 |
| | | | | Precision | 0.91 | 0.92 | 0.99 |
| | | | | Specificity | 0.955 | 0.962 | 0.991 |
| Experiment 2: Pixel Mapping + Proposed CNN | 96.13 | 96.08 | 93.92 | Sensitivity | 0.95 | 0.96 | 0.97 |
| | | | | Precision | 0.9 | 0.97 | 1 |
| | | | | Specificity | 0.984 | 0.964 | 0.988 |
| Proposed: Pixel Mapping → 2D DWT + CNN | **96.9** | **96.55** | **95.16** | Sensitivity | 0.93 | 0.98 | 0.99 |
| | | | | Precision | 0.95 | 0.96 | 1 |
| | | | | Specificity | 0.976 | 0.981 | 0.995 |

Consequently, we consider the model at epoch 61 as our best-performing one. A visual representation of the training progress in terms of epochs versus accuracy and loss is illustrated in Fig. 6.

TABLE IV
CONFUSION MATRIX OF THE PROPOSED MODEL

| Label | | Predicted | | |
|---|---|---|---|---|
| | | Meningioma | Glioma | Pituitary |
| True | Meningioma | 144 | 11 | 0 |
| | Glioma | 6 | 276 | 0 |
| | Pituitary | 2 | 0 | 174 |

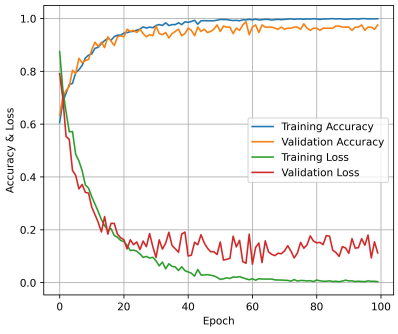


Fig. 6. Training-Validation Accuracy and Loss Curve

To assess the generalization capability of our model, we evaluated it on a separate test dataset, achieving an outstanding accuracy of 96.9%. We further computed the Kappa score, which yielded a highly respectable value of 95.16%. In addition, we conducted a comprehensive evaluation, including the calculation of precision, sensitivity, and specificity for each class, as detailed in Table III. And the confusion matrix is shown in Table IV.

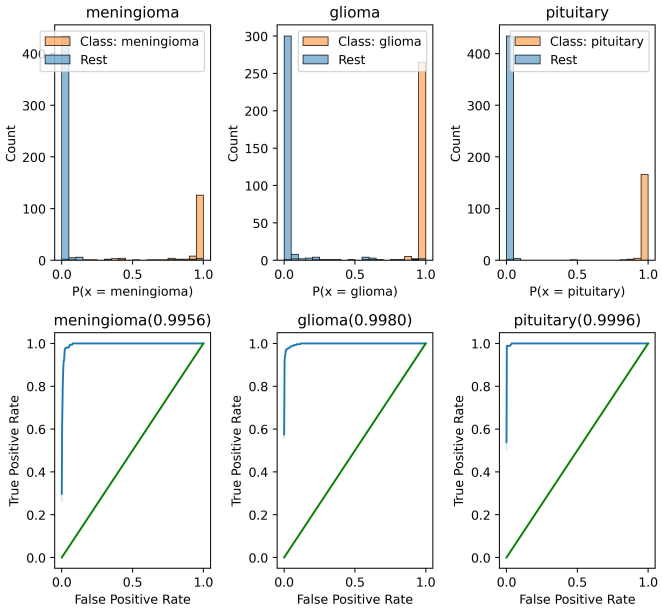


Fig. 7. ROC Curve Obtained from The Proposed Model

To benchmark our approach, we compared our results with those of five other methods proposed by the authors mentioned in Table III. Tonmoy et al. [7] originally developed their method and evaluated it on the BRATS dataset, designed for binary classification. In our study, we adapted their method

for experimentation with the figshare multiclass brain tumor dataset [8], providing a valuable comparison point. We also explored the method proposed by Das et al. [4]. Notably, we observed a slight improvement in accuracy when we modified the pixel scaling approach, deviating from their original pixel saturation technique.

Furthermore, we conducted an experiment using our own proposed CNN architecture. This approach involved scaling the pixels, resizing the images, and training the CNN. Impressively, our results yielded a 96.13% accuracy rate and a Kappa score of 93.92%, demonstrating its competitiveness with our primary proposed approach.

Fig. 7 illustrates the Receiver Operating Characteristic (ROC) curves for One versus Rest (OvR) Area Under the Curve (AUC) and presents a histogram. The degree of separability in the histogram provides insights into the model's accuracy. When the histogram exhibits clear separations between classes, it indicates that the model is accurate in distinguishing those classes. Conversely, if there is a significant overlap in the histogram, it suggests that the model faces challenges in identifying certain classes.

In Fig. 7, we can observe that the model performs exceptionally well in identifying the "Pituitary" class. This excellent performance is further corroborated by the data in Table III, which indicates the highest precision value of 1.00 for this particular class. However, the AUC score of Meningioma, Glioma, and Pituitary was found 0.9956, 0.9980, and 0.9996 respectively. And the average score was 0.9977.

## IV. Conclusion

In conclusion, accurate classification of brain tumors is of paramount importance in the realm of medical diagnostics and treatment planning. Our proposed image classification methodology represents a significant advancement in this critical area. The necessity for precise brain tumor identification stems from its direct impact on patient care, treatment decisions, and prognosis. The method's notable performance surpasses existing state-of-the-art techniques. This achievement can be attributed to its proficiency in addressing irregular pixel ranges, dimensionality reduction, and its ability to learn intricate features through CNNs. These outcomes underscore the robustness of our approach and its potential for broader medical applications. Looking forward, our research will focus on integrating transfer learning models to reduce computation time while further enhancing accuracy. This future direction aligns with our commitment to advancing medical image classification, ultimately contributing to more timely and precise diagnoses for improved patient outcomes.

## References


[1] A. C. Society, "Key statistics for brain and spinal cord tumors," 2023. Accessed: 2023-09-08.

[2] C. E. Board, "Brain tumor: Statistics," 2020. Accessed: 2023-09-08.

[3] T. B. T. Charity, "Statistics about brain tumours," 2021. Accessed: 2023-09-08.

[4] S. Das, O. F. M. R. R. Aranya, and N. N. Labiba, "Brain tumor classification using convolutional neural network," in *2019 1st International Conference on Advances in Science, Engineering and Robotics Technology (ICASERT)*, pp. 1–5, 2019.

[5] Z. A. Sejuti and M. S. Islam, "An efficient method to classify brain tumor using cnn and svm," in *2021 2nd International Conference on Robotics, Electrical and Signal Processing Techniques (ICREST)*, pp. 644–648, 2021.

[6] Z. N. K. Swati, Q. Zhao, M. Kabir, F. Ali, Z. Ali, S. Ahmed, and J. Lu, "Brain tumor classification for mr images using transfer learning and fine-tuning," *Computerized Medical Imaging and Graphics*, vol. 75, pp. 34–46, 2019.

[7] T. Hossain, F. S. Shishir, M. Ashraf, M. A. Al Nasim, and F. Muhammad Shah, "Brain tumor detection using convolutional neural network," in *2019 1st International Conference on Advances in Science, Engineering and Robotics Technology (ICASERT)*, pp. 1–6, 2019.

[8] J. Cheng, "brain tumor dataset," 4 2017.

[9] P. Kumar Mallick, S. H. Ryu, S. K. Satapathy, S. Mishra, G. N. Nguyen, and P. Tiwari, "Brain mri image classification for cancer detection using deep wavelet autoencoder-based deep neural network," *IEEE Access*, vol. 7, pp. 46278–46287, 2019.

[10] D. Barboriak, "Data from rider neuro mri." The Cancer Imaging Archive, 2015.

[11] M. T. Islam, M. Kumar, M. R. Islam, and M. Sohrawordi, "Subgrouping-based nmf with imbalanced class handling for hyperspectral image classification," in *2022 25th International Conference on Computer and Information Technology (ICCIT)*, pp. 739–744, 2022.

[12] M. R. Islam, M. T. Islam, and M. P. Uddin, "Improving hyperspectral image classification through spectral-spatial feature reduction with a hybrid approach and deep learning," *J. Spat. Sci.*, pp. 1–18, 2023.

[13] M. T. Islam, M. R. Islam, M. P. Uddin, and A. Ulhaq, "A deep learning-based hyperspectral object classification approach via imbalanced training samples handling," *Remote Sens. (Basel)*, vol. 15, no. 14, p. 3532, 2023.

[14] International Agency for Research on Cancer, "Iarc - bangladesh fact sheet," 2023.

[15] Y. Fan, X. Zhang, C. Gao, S. Jiang, H. Wu, Z. Liu, and T. Dou, "Burden and trends of brain and central nervous system cancer from 1990 to 2019 at the global, regional, and country levels," *Archives of Public Health*, vol. 80, no. 1, p. 209, 2022.

[16] Z. Khazaei, E. Goodarzi, V. Borhaninejad, F. Iranmanesh, H. Mirshekarpour, B. Mirzaei, H. Naemi, S. M. Bechashk, I. Darvishi, R. Ershad Sarabi, and A. Naghibzadeh-Tahami, "The association between incidence and mortality of brain cancer and human development index (hdi): an ecological study," *BMC Public Health*, vol. 20, no. 1, p. 1696, 2020.

[17] J. Seetha and S. S. Raja, "Brain tumor classification using convolutional neural networks," *Biomedical & Pharmacology Journal*, vol. 11, no. 3, p. 1457, 2018.

[18] P. K. Chahal, S. Pandey, and S. Goel, "A survey on brain tumor detection techniques for mr images," *Multimedia Tools Appl.*, vol. 79, p. 21771–21814, aug 2020.

[19] J. Cheng, W. Huang, S. Cao, R. Yang, W. Yang, Z. Yun, Z. Wang, and Q. Feng, "Enhanced performance of brain tumor classification via tumor region augmentation and partition," *PLOS ONE*, vol. 10, pp. 1–13, 10 2015.

[20] J. Cheng, W. Yang, M. Huang, W. Huang, J. Jiang, Y. Zhou, R. Yang, J. Zhao, Y. Feng, Q. Feng, and W. Chen, "Retrieval of brain tumors by adaptive spatial pooling and fisher vector representation," *PLOS ONE*, vol. 11, pp. 1–15, 06 2016.

[21] G. R. Lee, R. Gommers, F. Waselewski, K. Wohlfahrt, and A. O. Leary, "Pywavelets: A python package for wavelet analysis," *Journal of Open Source Software*, vol. 4, no. 36, p. 1237, 2019.

[22] K. Ananda Kumar, A. Prasad, and J. Metan, "A hybrid deep cnn-cov-19-res-net transfer learning architype for an enhanced brain tumor detection and classification scheme in medical image processing," *Biomedical Signal Processing and Control*, vol. 76, p. 103631, 2022.

[23] H. Mehnatkesh, S. M. J. Jalali, A. Khosravi, and S. Nahavandi, "An intelligent driven deep residual learning framework for brain tumor classification using mri images," *Expert Systems with Applications*, vol. 213, p. 119087, 2023.